INTERNATIONAL JOURNAL OF SCIENCE AND NATURE

www.scienceandnature.org

APPLICATION OF SUPERVISED ENHANCEMENT TECHNIQUE FOR CROP LAND MAPPING FROM LANDSAT DIGITAL DATA- A CASE STUDY ON BARDHAMAN BLOCK, BARDHAMAN DISTRICT,WEST BENGAL, INDIA

[1]Ratnadeep Ray, [2]Saptarshi Mondal, [3]Sakti Mandal
[1]Department of Remote Sensing and GIS, Vidyasagar University, Midnapore (West), West Bengal,
[2]Department of Remote Sensing and GIS, BIT, Mesra, Ranchi, Jharkhand,
[3]Department of Geography, University of Calcutta, Kolkata, West Bengal.

ABSTRACT
The enhancement technique is basically done for the betterment of image interpretability and analysis. This may be statistical or object oriented. For the study like change detection or object dynamics, object oriented enhancement should be given importance. The object oriented enhancement can be said as supervised enhancement which like the point operation, is the combination of spectral bands using algebraic operation from mathematical or algebraic functions by which selected target spectral features can be enhanced. In this present study a new object oriented enhancement algorithm has been proposed and a raster codification technique has been done to monitor the cropland type i.e. single, double, multiple etc within Bardhaman block of Bardwan district and has been applied on multi-seasonal digital database to get the typification of the croplands. Finally the distribution pattern of the crop land type has been experienced.

KEY WORDS: Supervised Enhancement, NDVI.

INTRODUCTION

Low sensitivity of the detectors, weak signal of the objects and the environmental conditions at the time of recording are the major causes of low contrast. Besides sometimes human eye acts poorly at discriminating the small radiometric or spectral differences, that may characterize the features. The main aim of the digital image enhancement is to amplify these least differences for better clarity of the scene. This means the digital image enhancement increases the separately between the nearly classes or features. It is basically a mathematical operation applied to the digital image to improve the visual appearance for better interpretability and subsequent digital analysis (Lillesand & Kifer, 1999). In remote sensing image processing, different kinds of digital enhancement algorithms are used like, contrast stretching, filtering, rationing, PCA, linear combinations, spectral band combination etc. Out of them some are statistical where the original histograms of the images are directly modified or some are object oriented where spectral band combinations are done using algebraic operations from mathematical and algebraic functions by which selected target spectral features can be enhanced. In the context of the present study, the object oriented enhancement algebraically can be considered as supervised enhancement as it is done on the basis of the prior spectral designations. By this objects' internal characteristics can be expressed as well as the separately can be recognized from the nearly spectral objects. In this present study this kind of enhancement algorithm seems very fruitful. Agricultural is the backbone of Indian economy, providing livelihood to about 67.0 per cent of the population and approximately 35.0 per cent to the Gross National Product. Food grain production has increased from 51 million tons in 1951 to 230.67 million tons in 2007-08. On the other end, the Indian population crossed the billion marks and needs around 250 million tons of food grains and calling for efficient agricultural management involving appropriate application of production and conservation practices for development of land and water resources on a sustainable basis. Substantial increase in crop production is possible by bringing additional land under cultivation (horizontal approach) and improved crop management (vertical approach) technologies such as use of high yielding input responsive, energy intensive and stress tolerant varieties, increased irrigation and integrated crop nutrition and protection. In addition, reliable and timely estimates and seasonal crop acreage and production estimates are important for formulation of marketing strategies such as export/import, price fixation, and public distribution. Conventional techniques to provide this information are highly tedious, time consuming more often subjective, whereas satellite remote sensing has the requisite potential to provide this information on a regular, synoptic, temporal, timely and in a more objective manner.

The remarkable developments in space borne remote sensing (RS) technology and its applications during the last three decades have firmly established its immense potential for mapping and monitoring of various natural resources. Remote Sensing can be defined as the science and art of acquiring information about objects from measurements made from a distance, without coming into physical contact of the object. Human eye, cameras and scanners are some of the examples. Satellite remote sensing and Geographic Information System (GIS) offer great promise for natural resources management with the ability to depict the spatial

distribution of the extent and monitoring capability. These techniques have potential to predict and zonate different levels of crop response to the inputs and can also provide solutions to various management problems in increasing the performance of the cropping system in a spatial and temporal dimension, when coupled with the relevant ancillary information. A suitable blend of these technologies aid in efficient management of our resources to enhance the crop productivity on a sustainable basis.

STUDY AREA

Bardhaman district is situated in the thick alluvial plain of Damodar river. The district is distinguished by the existence of both agricultural and industrial economy. The area, Bardhaman Sadar subdivision (fig.1), chosen for the present study is mainly agricultural based subdivision of Bardhaman district. Rice is richest crop among Wheat, Jute, Mung, Dal, Mustard seed. It's located between latitude N 22°55′55″ to N 23°37′05″ and longitude E 87°28′24″ to E 88°14′00″, in the middle of Bardhaman district. The total area covers approximately 3150 sq KM.

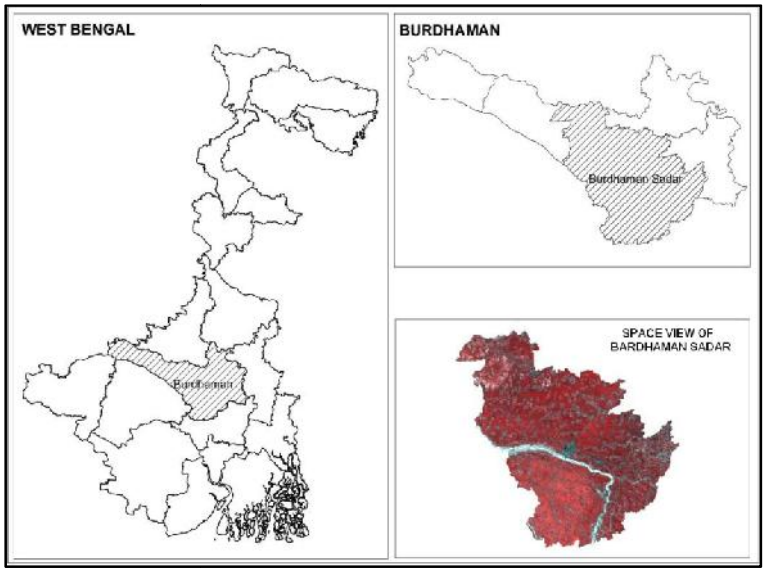

FIGURE 1. Location map of the study area

MATERIALS AND METHODS

For the current study Landsat TM5 data (path 139 row 44) of dated 24.10.2009, 13.2.2010 and 2.4.2010 has been used and has been processed in TNT mips pro and Arc GIS environment. The use of multi-temporal satellite data at a large scale using TM and ETM+ possesses a number of challenges including geometric correction error, noise arising from atmospheric effect, errors arising from changing illumination geometry, and instrument errors (Homer *et al*., 2004). Such errors can introduce biases in mangrove forest classification and change analysis. To reduce the noise due to influence of the atmospheric and illumination geometry, we used the techniques developed for the National Land Cover Database of the United States (Homer *et al*., 2004). Each image was normalized for variation in solar angle and Earth-sun distance by converting the digital number values to the top of the atmosphere reflectance (Chander and Markham, 2003). Considering the relative uncertainty of algorithms currently available, atmospheric correction was not performed. Only first-order normalization conversion to at-satellite reflectance was performed. This conversion algorithm is ''physically based, automated, and does not introduce significant errors to the data'' (Huang et al., 2002). In an image we can assume two type of pixel is presents, one is vegetation pixel and another is non-vegetation pixel. For vegetative pixel due to chlorophyll content there is significant difference in both absorption and reflectance of electromagnetic radiation in Green, Red and Near Infra Red (NIR) region. In vegetative pixel reflectance of Near Infra Red (NIR) band always will be greater than Red band. Based on these properties various multispectral indices or band ration already developed. An ideal vegetation index would be highly sensitive to vegetation and insensitive to soil-background changes and slightly influenced by atmospheric path radiance (Jackson *et al.,* 1983).

In this study an effort has been made for discriminating vegetative pixel and non-vegetative pixel from an image directly using Red and Near-infrared band of TM5 sensor firstly and after this using the nature of vegetation response to NIR and Red band of the spectrum actual agricultural crops are going to be discriminated form the plot margin vegetables/vegetations. Some consideration has been taken for developing the algorithm. As per figure 2-

1. Pixel value having chlorophyll influence will be greater in near-infrared band than red band.
2. Pixel value having no chlorophyll influence will be greater in red band than near-infrared band.
3. Pixel having same value in red and near infrared band and nearly positive or negatively correlated pixel in RED-NIR feature space will be considered as bare soil pixel (those pixel falling within a certain buffer distance of soil line in RED-NIR feature space).

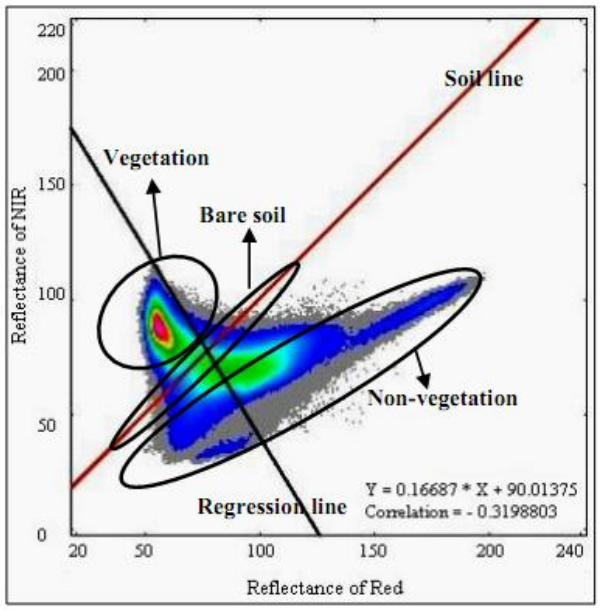

FIGURE 2. NIR and Red band feature space

Discriminating vegetative pixel from image

According to consideration No.1, from simple subtraction or ratio of NIR and Red band we can get vegetative pixel as a high positive value, but anyhow negative value is not be accepted in the pixel though negative value express some useful relevant information. So to avoid negative value and simultaneously to extract only vegetative pixel following algorithm has been developed -

$3*[\{(\rho NIR + L) * (255 - \rho RED)\} * (\rho NIR - \rho RED)]^{(1/2)}$ …….. (1)

(Where, ρRED = Reflectance value of Red band of TM5 Sensor, ρNIR = Reflectance value of Near-infrared band of TM5 Sensor, L= Coefficient - varies with the vegetation cover, Here L=2,

Value 255 is used to avoid negative pixel value which will convert as null cell in output.)

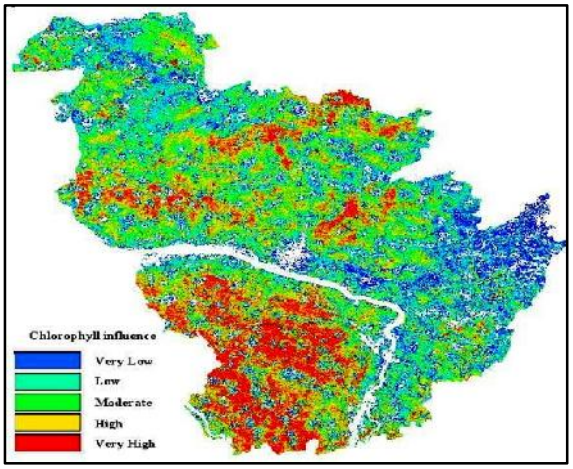

FIGURE 3. Supervised enhanced image showing vegetation coverage

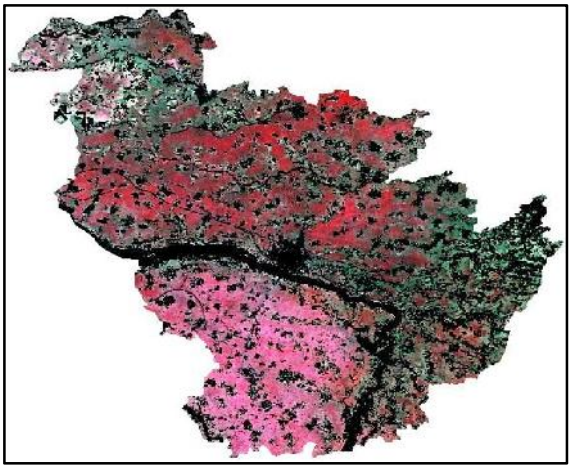

FIGURE 4. Vegetation FCC according to the supervised enhanced binary image

Discriminating non-vegetative pixel from image

In similar way according to consideration No.2, for bare soil, wet land, water body reflectance of red band is always greater from near infrared band. So the reverse form of equation no. 1 could be a meaningful way for discriminating non-vegetation pixel.

$3*[\{(\rho RED + L) * (255 - \rho NIR)\} * (\rho RED - \rho NIR)]^{(1/2)}$ …….. (2)

(Where, ρRED = Reflectance value of Red band of TM5 Sensor, ρNIR = Reflectance value of Near-infrared band of TM5 Sensor, L= Coefficient - varies with the vegetation cover, Here L=2.)

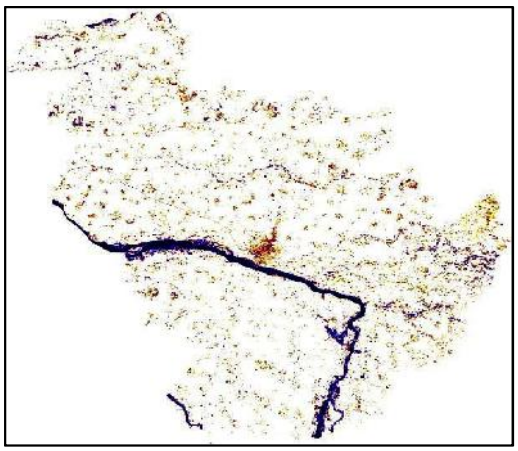

FIGURE 5. Supervised enhanced image showing non-vegetation coverage

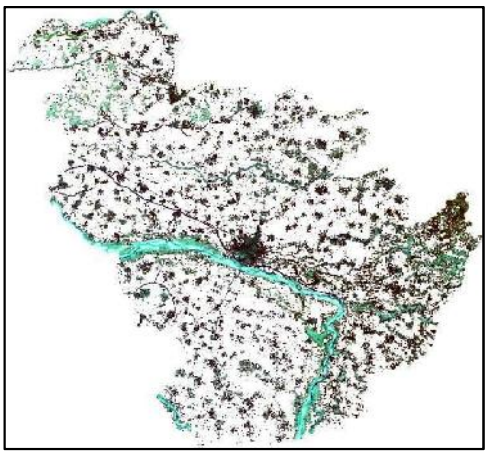

FIGURE 6. Non-Vegetation FCC according to the supervised enhanced binary image

Discriminating agricultural crop pixel from image

In case of discriminating the agricultural land having crop growth, the main problem arises with the background soil noise factors and the plot margin vegetables/ vegetations. In addition to the soil brightness, the soil colour may influence the vegetation index e.g. it can suppress the information. Escadafal and Huete (1991) developed a coloration index, the 'redness index' (RI) which is the correction factor for the soil colour effect on the vegetation indices. They found that the variations caused by soil colour greatly hinder the detection of vegetative colour rates. This factor comes in second place after soil brightness. The soil coloration index is thus a correlation permitting to double the sensitivity of vegetation indices. This index can be defined by following equation:

RI = (R-G)/(R+G) …… (3)

(Where the R and G are the mean reflectance of Red and Green channels respectively.)

The information provided by the green channel was used for correcting vegetation indices from the noise associated with the soil colour. The slope 'k' of the linear correlation between RI and the vegetation index for obtaining a corrected vegetation index (VI_{cor}) will be.

VI_{cor} = (VI-k*RI)…….. (4)

In the present study putting the output of equation.1 in place of VI of equation 4, we have got the corrected floristic information and for non-floristic coverage equation.2 has been used in equation 4 in the same manner.

The agricultural cropland can be discriminated on the basis of calculating the FMC (Fuel moisture content) and EWT (Equivalent water thickness). The EWT is the leaf water content and the FMC is the moisture content expressed in quantity of dry matter (%), which depends on both of EWT and dry matter (DM). So it can be said that both of these are nearly analogous. FMC modeling should be focused on the use of the NIR, SWIR wavelengths or water indices derived from spectral reflectance in those regions. TM/ETM+ has one band in NIR region located in 0.76– 0.90 mm (band4) and two bands in SWIR domain ranging from 1.55 mm to 1.75 mm (band5) and 2.09–2.35 mm (band7). Elvidge and Lyon (1985) showed that there were significant correlations between EWT and reflectance of both band5 and band7 but the strongest with band5 and suggested the combination of band 5 and band7 in a simple ratio to monitor vegetation water content. It was also reported by Chuvieco et al. (2002) that TM band5 was more strongly correlated with FMC than band7. NIR reflectance increases while SWIR decreases with the coupled effect of increased canopy EWT and decreased soil information viewed by the sensor.

NIR–SWIR reflectance space manifested itself in an approximate trapezoidal shape, was obtained (Fig. 7.A, B, C). It is worth noting that, reflectance in both NIR and SWIR are greater than the other 2 season, this may due to the irrigation activity and rainfall that fell before and after the irrigation term. Careful examination of the distribution features of surface targets on the scatter plot indicates that it follows certain distribution rules (fig.7.D). There is a baseline similar with soil line in NIR–red scatter plots; we name this line CD as NIR– SWIR base line, which represents the moisture status of the bare surface. Because FMC is related only with fully and partly vegetated area, pure pixels corresponding to water were removed, consequently, a hypothetical trapezoid was delineated as it can be seen in Fig. 4. Vertex n (n = A, B, C, D) inFig. 4 corresponds full cover with high canopy water content (EWT), full cover with low canopy water content (EWT), saturated bare soil and dry bare soil, respectively. Namely, as we have seen, CD shows the direction of bare surface stress severity. The direction orthogonal to NIR–SWIR base line represents the change of surface vegetation fraction cover from bare soil, partial cover and full cover. The vector of canopy water change is orthogonal to the NIR–SWIR base line, namely, the farther the distance is from the NIR–SWIR base line, the greater the amount of canopy EWT. Plots E and F represent partial cover with equal vegetation fraction.

SWIR increases due to leaf EWT decreases along the EF line. According to Ghulam et al. (2007), TM/ETM+ NIR band is not affected by EWT, and NIR reflectance should remain constant as a parallel line to the abscissa. However, a decrease is also evident in NIR with the increasing of the EWT. It is interesting to note that FMC varies along the lines AB and EF, namely, FMC decreases along the AB and EF lines as a possible result of decreased EWT with soil moisture depletion. CA and DB describe the maximal and minimal water lines in the NIR–SWIR spectral space. Finally it is explored that the pure crop pixels are staying at the vertex B of the Trapezoid and those are collected as the spectral end member from the output raster of the joint product of equation 1and 4. All the calculations and experiments are done for the images of kharif, rabi and zaid season to show the distribution of agricultural cropland distribution. After this those three seasonal cropland layers have been converted to binary having the values of 1 and 0 and have been multiplied with 1;10;100 respectively and are combined in a linear fashion following the equation,

Crop land type = ∑Cn*c …….. (5)

(Where, Cn= each season; c= coefficients like 1, 10,100)

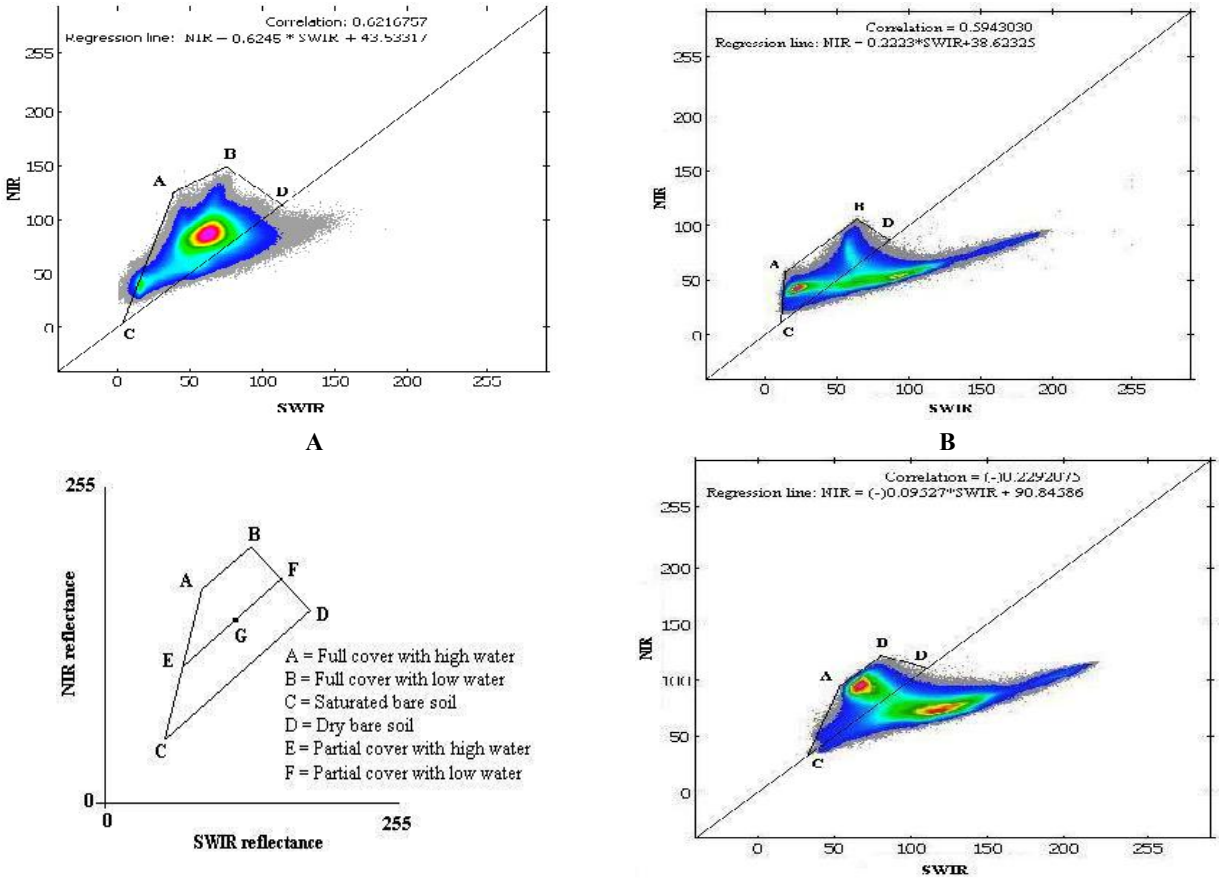

FIGURE 7. (A, B, C) Spectral plots of NIR against SWIR over Bardhaman Sadar block; (D) Sketch map of vegetation pixel location.

RESULT AND DISCUSSION

It is previously said that the supervised enhancement is important to enhance a specific spectral target using a specific band combination following algebraic and mathematical functions. In this present study for delineating floristic spectral behavior a new linear band combination (equation 1) has been applied where the NIR response has been made free from coloration effects of soil and BDRF using equation 4. In different literature it has been established that for NIR and Red spectral space the spectrum having floristic information will stay above the soil line and for the case of non-floristic spectra it will be vice versa. In this present study the NIR and Red band spectral information of the floristic and non-floristic coverage (fig. 4 and 6) extracted using equation 4 is seen to follow that consideration (fig. 8 A and B). Within the extracted vegetal coverage there exists the mixed spectral information for the crop and the plot margin vegetables/ vegetation and the main problem arises with this. It has been experimented that for the agricultural crop has the low EWT and FMC than the plot margin vegetables/ vegetation. So by demarcating these parameters the crop lands can be discriminated. Besides, the variations in horizontal density of the floristic species and the spectral variability in the NIR and the SWIR region can be considered as the determining factor for the crop lands. In figure 7, if the trapezoidal spectral plots for the vegetal coverage are carefully examined it is seen that for the kharif season both of NIR and SWIR region is higher than the other. This may be due to the irrigation activity and

high rainfall that fell before and after the irrigation term. So for the kharif season the spectral end members for the crop has been collected from point 'A' of the trapezoidal spectral plot (fig.7.A) and for the other two seasons the spectral end members have been collected for the crop from point 'B' (fig.7.B; C). After all these processes the crop pixel clusters have been converted to binary mask to get the symmetry in value for the further processing (fig.8.A;B).

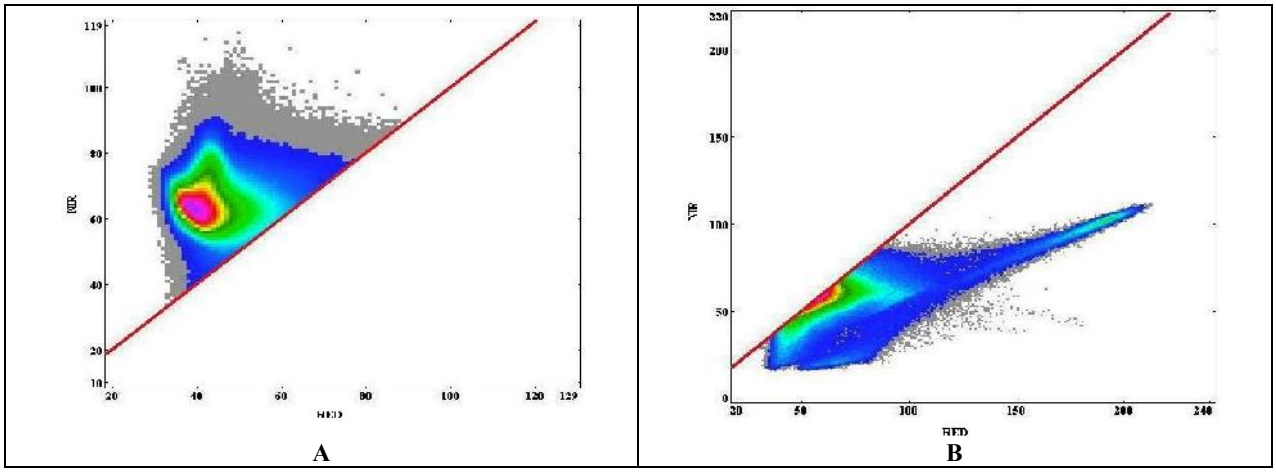

FIGURE 8. NIR and RED spectral plots of vegetation (A) and Non-vegetation (B) features

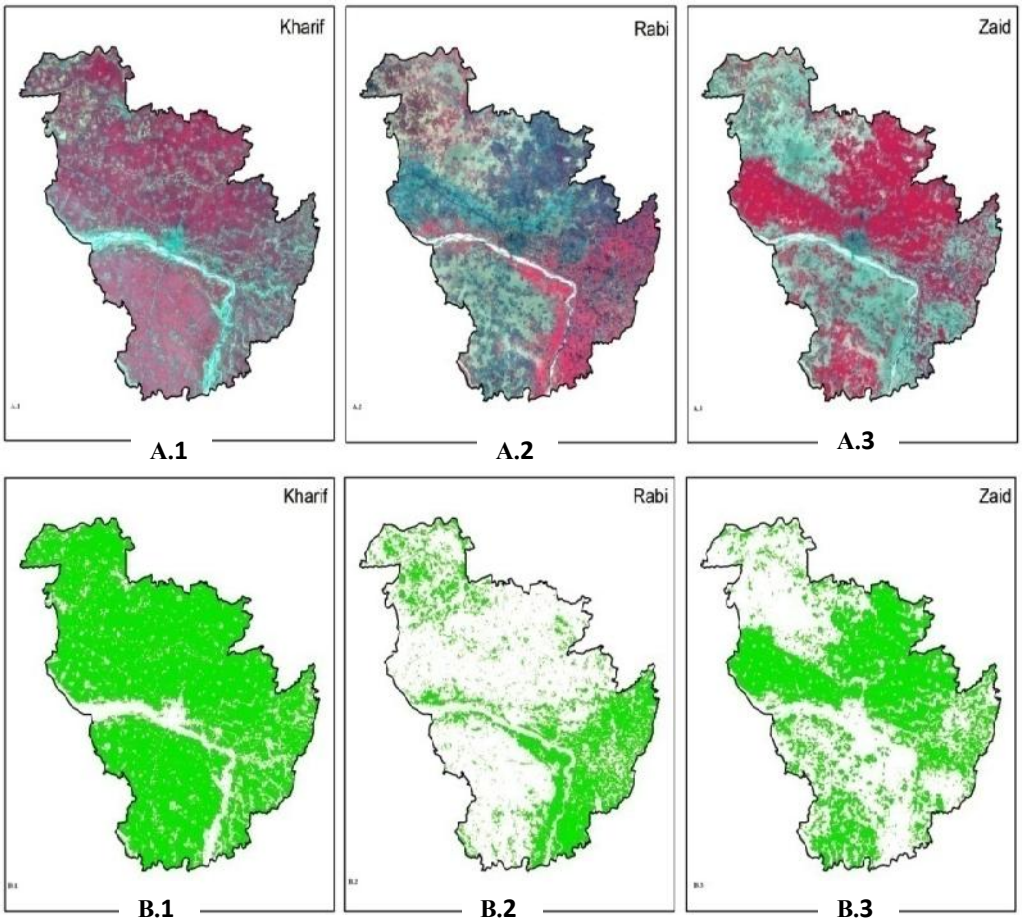

FIGURE 8. FCC of Kharif, Rabi and Zaid season (A.1, 2, 3); Binary mask of Kharif, Rabi and Zaid season according to spectral response of NIR and SWIR (B.1, 2, 3).

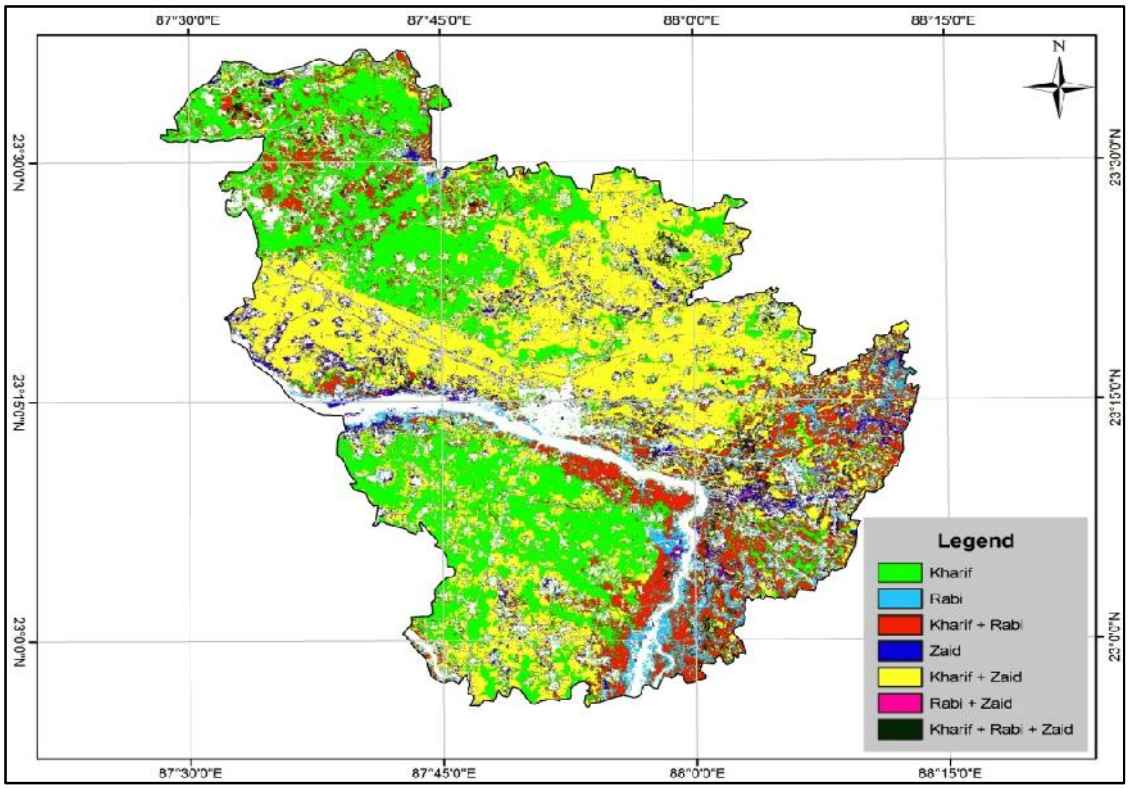

FIGURE 9. Map showing crop land types of Bardhaman Sadar block

Finally the linear combination of the three binary masks of the respective seasons following the equation 5 has produced the crop land type map (fig.9) from which different code type of values has depicted typical crop lands like 1, 10, 100 are Kharif, Rabi and Zaid crop lands which are of single crop land type; 110,101 are Kharif and Rabi crop lands which are double crop land type and 111 is Kharif, Rabi and Zaid crop land which are triple or multiple crop land.

CONCLUSION

After overall analysis and discussion, it can be concluded that for the environmental mapping and monitoring supervised enhancement can play an important role. Ample combinations of algebraic operations can be derived from basic arithmetic operations and algebraic functions. But aimless combinations of algebraic operations and arithmetic functions can not provide any satisfactory result though that may be visually impressive. So using the knowledge of the spectral properties of the target features, an effective and meaningful band combination algebraically can be designed to truly enhance the particular target. These kinds of algebraic band combination having supervised nature can also suppress image radiometric flaws and atmospheric scattering effects. In this present study by formulating a spectral indices based on the NIR and Red spectral property of vegetation, the health status as well as the density and distributional nature becomes so interpretable, that an environmentalist can undertake some effective decision for environmental sustainability and resource management.

REFERANCES

Allen, C.D., Breshears, D.D. (1998) Drought induced shift of a forest woodland ecotone: rapid landscape response to climate variation. Proc. Natl. Acad. Sci. U.S.A. 95 (25), 14839–14842.

Alves, I., Pereira, L.S. (2000) Non-water-stressed baselines for irrigation scheduling with infrared thermometers: a new approach. Irrigation Sci. 19, 101–106.

Anatoly, A.G., Kaufman, Y.J., Stark, R., Rundquis, D. (2002) Novel algorithms for remote estimation of vegetation fraction. Remote Sensing of Environment 80 (l), 76–87.

Arnon, D.I. (1949) Copper enzymes in isolated chloroplasts polyphenoloxidae in Beta vulgaris. Plant. Physiol. 24, 1–15.

Asrar, G.F., Myneni, R.B., Choudhury, B.J. (1992) Spatial heterogeneity in vegetation canopies and remote sensing of absorbed photosynthetically active radiation: a modeling study. Remote Sensing of Environment 41, 85–103.

Bannari, A., Mori, D., Bonn, E. (1995) A review of vegetation indices. Remote Sensing Reviews 1995 (13), 95–120.

Boles, S.H., Xiao, X., Liu, J., Zhang, Q., Munkhtuya, S., Chen, S., Ojima, D. (2004) Land covers characterization of Temperate East Asia using multi-temporal

VEGETATION sensor data. Remote Sensing of Environment 90, 477–489.

Bonham, C. D. (1989) Measurements for Terrestrial Vegetation. Wiley, New York, p. 352.

Brazel, A.J., Nickling, W.G. (1987) Dust storms and their relation to moisture in the Sonoran-Mojave desert region of the south-western United States. Journal of Environmental Management 24, 279–291.

Chen, J. (1999) Spatial scaling of a remotely sensed surface parameter by contexture. Remote Sensing of Environment 69, 30–42.

Choudhury, B.J. (1987) Relationships between vegetation indices, radiation absorption and net photosynthesis evaluated by a sensitivity analysis. Remote Sensing of Environment 22 (2), 209–233.

Dunean, J., Stow, D., Franklin, J., Hope, A. (1993) Assessing the relationship between spectral vegetation indices and shrub cover in the Jornada Basin, New Mexico. International Journal of Remote Sensing 14 (18), 3395–3416.

Dymond, J.R., Stephens, P.R., Newsome, P.F. (1992) Percent vegetation covers of a degrading rangeland from SPOT. International Journal of Remote Sensing 13 (11), 1999–2007.

Elvidge, C.D., Lyon, R.J.P. (1985) Influence of rock-oil spectral variation on the assessment of green biomass. Remote Sensing of Environment 17 (3), 265–279.

Elvidge, C.D., Chen, Z. (1995) Comparison of broad-band and narrow-band red and near-infrared vegetation indices. Remote Sensing of Environment 54 (l), 38–48.

Ghulam, A., Li, Z.-L., Qin, Q., Tong, Q., Wang, J., Kasimu, A., Zhu, L. (2007) A method for canopy water content estimation for highly vegetated surfaces—shortwave infrared perpendicular water stress index. Sci. Chin. Ser. D: Earth Sci. 50, 1359–1368.

Godínez-Alvarez, H., Herrick, J.E., Mattocks, M., Toledo, D., van Zee, J. (2009) Comparison of three vegetation monitoring methods: their relative utility for ecological assessment and monitoring. Ecological Indicators 9 (5), 1001– 1008.

Gooding, M.J., Ellis, R.H., Shewry, P.R., Schoeld, J.D. (2003) Effects of restricted water availability and increased temperature on the grain filling, drying and quality of winter wheat. J. Cereal Sci. 37, 295–309.

Graetz, R. D., Pech, R.R., Davis, A.W. (1988) The assessment and monitoring of sparsely vegetated rangelands using calibrated Landsat data. International Journal of Remote Sensing 9 (7), 1201–1222.

Gutman, G., Lgnatov, A. (1998) The derivation of the green vegetation fraction from NOAA/AVHRR data for use in numerical weather prediction models. Interna-tional Journal of Remote Sensing 19 (8), 1533–1543.

Hardisky, M.A., Klemas, V., Smart, R.M. (1983) The influence of soil salinity, growth form, and leaf moisture on the spectral radiance of Spartina alterniflora canopies. Photogr. Eng. Remote Sens. 49, 77–83.

Huete, A.R. (2004) Remote sensing of soils and soil processes. In: Ustin, S.L. (Ed.), Remote Sensing for Natural Resource Management and Environment Monitoring. Manual of Remote Sensing, vol. 4, 3rd edition. John Wiley & Sons, Inc, Hoboken, NJ, USA, pp. 3–52.

Hunt, E.R., Rock, B.N., Nobel, P.S. (1987) Measurement of leaf relative water content by infrared reflectance. Remote Sens. Environ. 22, 429–435.

Jiang, Z., Huete, A.R., Chen, J., Chen, Y., Li, J., Yan, G., Zhang, X. (2006) Analysis of NDVI and scaled difference vegetation index retrievals of vegetation fraction. Remote Sensing of Environment 101, 366–378.

Jing, X., Yao, W., Wang, J., Song, X. (2010) A study on the relationship between dynamic change of vegetation Coverage and precipitation in Beijing's moun-tainous areas during the last 20 years. Mathematical and Computer Modelling, 1–7.

Kutiel, P., Cohen, O., Shoshany, M., Shub, M. (2004) Vegetation establishment on the southern Israeli coastal sand dunes between the years 1965 and 1999. Landscape and Urban Planning 67 (1–4), 141–156.

Leprieur, C., Verstraete, M., Pinty, B. (1994) Evaluation of the performance of vari-ous vegetation indices to retrieve vegetation cover from AVHRR data. Remote Sensing Reviews 10, 265–284.

Li, Z., Li, X., Wei, D., Xu, X., Wang, H. (2010) An assessment of correlation on MODIS-NDVI and EVI with natural vegetation coverage in Northern Hebei Province, China. Procedia Environmental Sciences 2, 964–969.

Muller-Dombois, D., Ellenberg, H. (1974) Aims and Methods of Vegetation Ecology. Wiley, New York, p. 80.

Neigh, C.S.R., Tucker, C.J., Townshend, J.R.G. (2008) North American vegetation dynamics observed with multi-resolution satellite data. Remote Sensing of Envi-ronment 112 (4), 1749–1772. North,

Price, J.C. (1992) Estimating vegetation amount from visible and near infrared reflectance. Remote Sensing of Environment 41, 29–34.

Purevdor, J.T.S., Tateishi, R. Ishiyama, T. (1998) Relationships between percent vege-tation cover and vegetation indices. International Journal of Remote Sensing 19 (18), 3519–3535.

Quamby, N.A., Townshend, J.R.G., Settle, J.J. (1992) Linear mixture modeling applied to AHVRR data for crop

area estimation. International Journal of Remote Sensing 13 (3), 415–425.

Ray. R., Paul, A.K., Basu, B. (2013) Application of Supervised Enhancement Technique in Monitoring the Mangrove Forest Cover Dynamics – A Case Study on Ajmalmari Reserve Forest, Sundarban, West Bengal, International Journal of Remote Sensing and Geoscience.vol.3, issue 1,pp. 16-21.

Ray. R., Mondal, S., Dutta, A. (2013) Application of Liner Spectral Mixing Model in Fractional Vegetation Cover Mapping - A case study on part of Jungle Mahal Region, West Bengal, India. International Journal of Science and Nature. (In press).

Senseman, G. M., Bagley, C.F., Tweddale, S.A. (1996) Correlation of rangeland covers measure to satellite-imagery-derived indices. Geocarto International 11, 29–37.

Shoshany, M., Kutiel, P., Lavee, H. (1996) Monitoring temporal vegetation cover changes in Mediterranean and arid ecosystems using a remote sensing tech-nique: case study of the Judean Mountain and the Judean Desert. Journal of Arid Environments 33, 9–21.

Steffen, W. (2003) The IGBP terrestrial transects: Tools for resource management and global change research at the regional scale. In: Ringrose, S., Chanda, R. (Eds.), Towards Sustainable Management in the Kalahari Region: Some Essential Background and Critical Issues. , pp. 1–11.

Sykioti, O., Paronis, D., Stagakis, S., Kyparissis, A. (2011) Band depth analysis of CHRIS/PROBA data for the study of a Mediterranean natural ecosystem: cor-relations with leaf optical properties and ecophysiological parameters. Remote Sensing of Environment 115 (2011), 752–766.

Tammervik, H., Hogda, J.A., Solheim, I. (2003) Monitoring vegetation changes in Pasvik (Norway) and Pechenga in Kola Peninsula (Russia) using multitemporal Landsat MSS/TM data. Remote Sensing of Environment 85 (3), 370–388.

Verstraete, M.M., LePrieur, C., De Brisis, S., Pinty, B. (1993) GEMI: a new index to estimate the continental fractional vegetation cover. In: Proceedings of the 6th AVHRR Data User's Meeting, Belgirate, Italy, 29 June–2 July, pp. 143–149.

Wang, G., Wente, S., Gertner, G.Z., Anderson, A. (2002) Improvement in mapping veg-etation cover factor for the universal soil loss equation by geostatistical methods with Landsat Thematic Mapping images. International Journal of Remote Sens-ing 23 (18), 3649–3667.

White, M.A., R.G. Asner, P.R. Nemani, J.L., Running, S.W. (2000) Measuring fractional cover and leaf area index in arid ecosystem: digital camera, radiation transmittance, and laser altimetry methods. Remote Sensing of Environment 74 (l), 45–57.

Wittich, K.P., Hansing, O. (1995) Area-averaged vegetative cover fraction estimated form satellite data. International Journal of Biometeorology 38 (3), 209–215.

Wu, J., Peng, D. (2010) A research on extracting information of the arid regions' vege-tation coverage using improved model of spectral mixture analysis. Multimedia Technology (ICMT), 1–5.

Zhou, Q. (1996) Ground truthing, how reliable is it? In: Proceedings of Geoinfor-matics'96 Conference, West Palm Beach, FL, 26–28 April. CPGIS, Berkeley, pp. 69–77.